Bioorganic & Medicinal Chemistry 20 (2012) 859–865

Contents lists available at SciVerse ScienceDirect

Bioorganic & Medicinal Chemistry

journal homepage: www.elsevier.com/locate/bmc

Studies on the biosynthesis of the lipodepsipeptide antibiotic Ramoplanin A2

Amanda J. Hoertz, James B. Hamburger, David M. Gooden, Maria M. Bednar, Dewey G. McCafferty *

Department of Chemistry, Duke University, Durham, NC 27708, USA

ARTICLE INFO

Article history:
Received 4 August 2011
Revised 22 November 2011
Accepted 28 November 2011
Available online 7 December 2011

Keywords:
Ramoplanin
Enduracidin
Non-ribosomal peptide synthesis
Antibiotic
Peptide

ABSTRACT

Ramoplanin, a non-ribosomally synthesized peptide antibiotic, is highly effective against several drug-resistant Gram-positive bacteria, including vancomycin-resistant *Enterococcus faecium* (VRE) and methicillin-resistant *Staphylococcus aureus* (MRSA), two important opportunistic human pathogens. Recently, the biosynthetic cluster from the ramoplanin producer *Actinoplanes* ATCC 33076 was sequenced, revealing an unusual architecture of fatty acid and non-ribosomal peptide synthetase biosynthetic genes (NRPSs). The first steps towards understanding how these biosynthetic enzymes cooperatively interact to produce the depsipeptide product are expression and isolation of each enzyme to probe its specificity and function. Here we describe the successful production of soluble enzymes from within the ramoplanin locus and the confirmation of their specific role in biosynthesis. These methods may be broadly applicable to the production of biosynthetic enzymes from other natural product biosynthetic gene clusters, especially those that have been refractory to production in heterologous hosts despite standard expression optimization methods.

1. Introduction

Natural product research has been transformed in recent years by the application of microbial genetics, improved genome sequencing methods, and bioinformatics. The rich chemistry of assembly of natural products is reflected in their unique chemical structures, but still the distinctive enzymatic transformations and the timing of assembly and modification are often nonobvious upon inspection of the biosynthetic locus sequence. Chemical biology studies of natural products biosynthesis have been historically plagued by technical problems associated with the production of enzymes from within biosynthetic loci. Many microorganisms that produce natural products are highly G+C rich, and as such cloning and expressing these gene products in heterologous organisms, including other antibiotic producing organisms has proved often problematic. When these genes can be expressed, it is common for the heterologous hosts to lack the chaperone machinery to correctly fold gene products into soluble and active enzymes.

Our ability to study natural product biosynthesis using chemical biology approaches requires the production of active enzymes and often the reconstitution of these activities in vitro. Furthermore, polyketide and non-ribosomal synthetases are exceptionally long, multidomain enzymes, often >100 kDa. Fragments of these enzymes lack the stability afforded by the remaining surrounding structure and thus often have impaired activity. Production of soluble, active biosynthetic enzymes has been an almost insurmountable barrier for the field, and as such restricts the breadth of analysis of natural product biosynthesis to the handful of amenable systems, such as deoxyerythronolide B synthetase (DEBS) for polyketides or enterobactin for NRPSs, for example.

Ramoplanin A2 is a 17-residue non-ribosomally produced lipoglycodepsipeptide antibiotic from *Actinoplanes* ATCC 33076 (Fig. 1).[1–4] Ramoplanin A2 exhibits activity against clinically-important Gram-positive bacteria including vancomycin-resistant *Enterococcus* sp. (VRE), methicillin-resistant *Staphylococcus aureus* (MRSA) and vancomycin-intermediate resistant *Clostridium difficile*.[1,5–12] Ramoplanin A2 inhibits peptidoglycan biosynthesis by interfering with the late-stage transglycosylation cross-linking reactions.[13,14] The mechanism involves sequestering Lipid Intermediate II, a key biosynthetic intermediate in peptidoglycan biosynthesis.[13,14] Capture of Lipid II physically occludes this substrate from proper utilization in downstream crosslinking reactions catalyzed by transglycosylases that produce mature peptidoglycan polymer, in turn affecting the mechanical integrity of the cell wall.

Recently, the 33 kb biosynthetic gene cluster from the ramoplanin producer *Actinoplanes* ATCC 33076 was sequenced by Farnet et al., revealing an unusual architecture of fatty acid and non-ribosomal peptide synthetase biosynthetic genes (NRPSs).[15] As shown in Fig. 2a, the ramoplanin biosynthetic gene locus contains 33 genes responsible for a myriad of functions including amino acid (Orfs 4, 6, 7, 28, 30), fatty acid (Orfs 9, 16, 24, 25, 26, 27) and peptide biosynthesis (Orfs 11, 12, 13, 14, 15, 17), polypeptide tailoring (Orfs 10, 20), antibiotic export/producer resistance (Orfs 2, 8, 23, 31), and transcriptional regulation (Orfs 5, 21, 22, 33).

* Corresponding author. Tel.: +1 919 660 1516; fax: +1 919 668 5483.
E-mail address: dewey.mccafferty@duke.edu (D.G. McCafferty).

0968-0896/$ - see front matter © 2011 Published by Elsevier Ltd.
doi:10.1016/j.bmc.2011.11.062

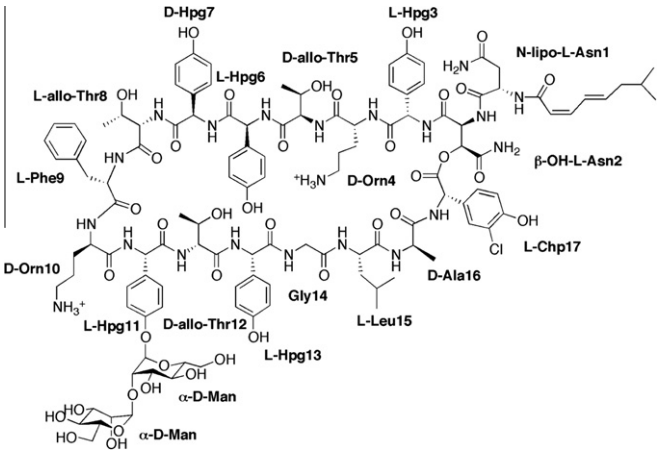

Figure 1. Structure of Ramoplanin A2.

The first unusual feature of the ramoplanin biosynthetic cluster stems from analysis of the four putative NRPS peptide synthetases, Ramo 12, 13, 14 and 17 (Fig. 2). Common to these synthetases are repeated modular defined domains that catalyze specific reactions of peptide synthesis.[16–18] The order of these domains within the enzyme determines the sequence and structure of the peptide product. For each amino acid in the peptide sequence, NRPS contain unique tri-functional modules comprised of condensation (C), adenylation (A), and thiolation (T) domains.[16] NRPS active sites of C, A, and T domains are highly organized so that a specific amino acid is recognized and incorporated into the peptide sequence.[19,20] Collectively there are 16 individual A domains that code for 16 of the 17 amino acids of ramoplanin (Fig. 2b). However, Ramo 12 contains the sole A domain with predicted specificity for asparagine and as such this domain is believed to catalyze the incorporation of both Asn[1] and β-OH-Asn[2] into the peptide chain.[21]

A second interesting aspect of this biosynthetic cluster is the predicted in trans mechanism of amino acid activation and condensation occurring between two NRPS synthetases.[21] Module 8, located in Ramo 13, is hypothesized to activate *allo*-Thr[8] and, possesses C and T domains but no A domain (Fig. 2). Interestingly, within Ramo 17 there exists a Thr-specific A domain, and as such Ramo 17 is predicted to interact with module 6 of Ramo 13 in trans to catalyze the incorporation of *allo*-Thr at the correct position.

A third feature of this cluster centers on the assembly of the starter unit. NRPS enzymes typically contain A domains at the start site, but the ramoplanin NRPS of Ramo 12 contains a C domain at its *N*-terminus prior to the module coding for Asn[1] activation and incorporation (Fig. 2).[21,22] This architecture suggests that the initiation of peptide synthesis may form from condensation of a fatty acid rather than an amino acid. One may speculate that a fatty acid adenylate, acyl-ACP or acyl-CoA may be the substrate for this C domain, catalyzing the *N*-acylation of Asn[1] and providing an intermediate for chain elongation by repeated condensation at the same site on Ramo 12 with β-OH-Asn[2] (or non-hydroxylated Asn) to produce the *N*-acyl-dipeptide starting unit.

This unusual NRPS architecture suggests possible functions for Ramo 9, 11, 15, and 26 for the activation and transfer of fatty acid precursors to the Ramo 12 peptide synthetase. Ramo 26 shares homology with acyl-CoA ligases, proteins that catalyze the activation of fatty acids via an activated adenylate intermediate. Ramo 11 is a putative acyl carrier protein (ACP) that accept activated adenylate intermediates and can be phosphopantetheinylated. It is hypothesized that Ramo 11 shuttles activated fatty acid thioesters to Ramo 12 that serve as the initiating groups for N-acylation of Asn[1]. Ramo 15 is a putative type II thioesterase that may play a role in acyl-ACP or acyl-coenzyme A (CoA) hydrolysis. Similarly, Ramo 9 appears to bear similarity to esterases of the alpha/beta hydrolase fold family. These enzymes may shuttle the fatty acid to the NRPS through enzyme acyl intermediates or may serve in a hydrolytic capacity to remove misprimed intermediates.

Lastly, Ramo 16, 24 and 25 are three proteins with homology to NADH and FAD-dependent enzymes involved in fatty acid metabolism. It is hypothesized that these proteins work to biosynthesize the N-terminal *cis*, *trans* 7-methyloctadienoic acid acyl chain.[21,23] Ramo 16 exhibits high similarity to NADH-dependent 3-oxoacyl acyl carrier protein reductases, which are involved in the degradation of fatty acids in primary metabolism and may reduce 3-oxoacyl-ACP (or 3-oxoacyl-CoA) to the corresponding 3-hydroxyacyl-ACP (or 3-hydroxyacyl-CoA).[16] Similarly, Ramo 24 and 25, proteins homologous to FAD-dependent acyl-CoA dehydrogenases

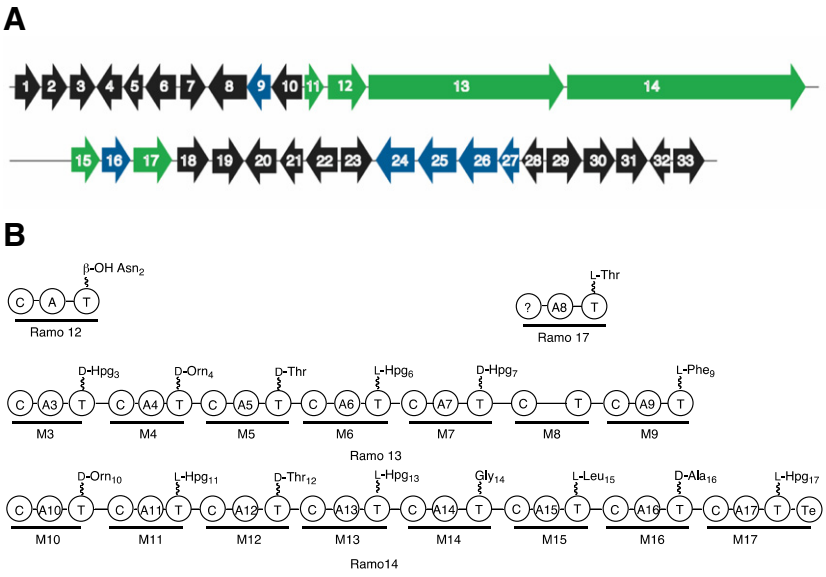

Figure 2. (A) Schematic of the genes composing the ramoplanin biosynthetic cluster. Genes implicated in fatty acid biosynthesis are colored in blue; genes associated with non-ribosomal peptide synthesis are shown in green; all other genes in the cluster are shown in black; (B) Organization and amino acid specificity of the condensation, adenylation, thiolation, and thioesterase subdomains within the four non-ribosomal peptide synthetase enzymes from the ramoplanin biosynthetic locus.

found in fatty acid biosynthesis, likely are responsible the regioselective dehydrogenation of 3-hydroxyacyl-ACP (or 3-hydroxyacyl-CoA) precursors.[21] It is not clear from primary sequence analysis if Ramo 24 or 25 catalyze regioselective dehydrations to produce uniquely *cis* versus *trans* olefins, but the presence of two genes and the two types of alkene regioisomers in the acyl chain is suggestive of a possible specialized role in this capacity.

One strategy to improve the production of soluble forms of mammalian and bacterial enzymes during heterologous expression in *Escherichia coli* is through co-expression with the protein folding chaperones. Very recently, Leadlay and coworkers demonstrated that co-expression of deoxyerythronolide B polyketide synthase (DEBS PKS) in the presence *Streptomyces coelicolor* chaperonins improved the activity of recombinant DEBS through increasing the fraction of correctly folded enzyme within the soluble protein produced.[24] Building on this and other precedents,[25–29] we report here the *Streptomyces lividans* GroEL/GroES1 chaperone-assisted production and functional characterization of several enzymes from the within the ramoplanin biosynthesic gene cluster.

2. Results and discussion

2.1. Coexpression of ramoplanin biosynthesis genes with GroES/GroEL improves soluble protein production

In preparation for these studies, expression plasmids were constructed to produce select ramoplanin biosynthetic enzymes as C-terminal hexahistidine fusion constructs. These plasmids were transformed into *E. coli* BL21 cells or *E. coli* BL21-RP cells (possessing the GC-rich tRNAs on a helper plasmid) alone and in combination with either the *E. coli* groES/groEL or the *S. lividans* groES/groEL1 expression plasmids. Identical growth and induction conditions were employed for each strain harboring an expression plasmid. Bacterial cultures uniformly were harvested and lysed, producing a soluble extract that was subjected to a standardized nickel–chelate affinity chromatography purification method to isolate each purified protein identically. Similarly, protein quantitation was standardized. Data indicating the relative amounts of soluble purified proteins produced in the presence of the *E. coli* and *S. lividans* chaperones are summarized in Table 1. Compared to the no chaperone control, co-expression with *E. coli* GroES/GroEL resulted in significant increases of the yield of soluble proteins for Ramo 9, 15, 26, and 27. No net increase was observed for Ramo 11 and 16, and the remainder of genes examined did not produce soluble proteins with the *E. coli* chaperones.

In contrast, switching to co-expression of the same genes in the presence of *S. lividans* GroES/GroEL1 chaperones significantly increased the yield of soluble proteins (Table 1). Yields ranging from 1 to 315 mg of proteins per liter were determined. Co-expression with the *S. lividans* GroES/GroEL1 plasmid increased soluble protein production levels dramatically, in most cases yields nearly doubled from co-expression with the *E. coli* chaperones and nearly tripled as compared to the no-chaperone control. In some cases, such as Ramo 17 and 24, soluble protein was produced for the first time.

2.2. Biological activity of select proteins from the ramoplanin biosynthetic locus

Nearly all of the proteins listed in Table 1 that produced soluble protein in the absence of either *E. coli* or *S. lividans* GroESL chaperones were nearly devoid of their anticipated enzymatic activity due in part to misfolding and long term aggregation encountered within the time course of purification. Co-expression in the presence of *S. lividans* GroES/GroEL1 proteins increased the amount of soluble protein. This allowed for the demonstration of some of the previously uncharacterized activities of ramoplanin biosynthesis enzymes and proteins such as Ramo 11 (a predicted acyl-carrier protein), Ramo 17 (a predicted NRPS enzyme containing a stand-alone adenylation–thiolation domain) and Ramo 16 (a predicted 3-oxoacyl-ACP reductase).

2.3. Phosphopantetheinylation of Ramo 11 by the *Bacillus subtilis* Sfp transferase

Ramo 11 is the putative acyl carrier protein (ACP) within the ramoplanin biosynthetic locus. During biosynthesis of the *N*-acyl 7-methyl-octadieneoic fatty acid, precursors are tethered to Ramo 11 via a thioester link and then the acyl–ACP is utilized as a substrate for either type II-like fatty acid biosynthesis modification enzymes like Ramo 16, 34, 25 etc. or for shuttling the acyl cargo to Ramo 12 for condensation with Asn[1] at the starter unit.[21] To produce a substrate competent for acylation, the *holo*-ACP form of Ramo 11 must be generated by primary metabolism phosphopantetheinyl transferases.[16] Recombinant Ramo 11 produced in *E. coli* is largely produced in the *apo* form because *E. coli* enzymes from fatty acid metabolism are still capable of transferring this cofactor to Ramo 11, albeit inefficiently. To examine if Ramo 11 was folded correctly following *S. lividans* GroES/GroEL1 co-expression, we tested its ability to undergo phosphopantetheinylation by the *B.*

Table 1
Expression yields of Ramoplanin biosynthetic proteins

Orf name	Putative function	No chaperone	GroESL plasmid from *E. coli* [c]	GroESL plasmid from *S. lividans*
Ramo 9[a]	Type II thioesterase	n. d. [c]	1.9 mg/L [d]	9.8 mg/L [d]
Ramo 11[a]	Acyl carrier protein	16 mg/L	—	16.8 mg/L
Ramo 12[a]	NRPS	n. d.	n. d.	n. d.
Ramo 12[b]		n. d.	n. d.	n. d.
Ramo 15[a]	Type II thioesterase	31 mg/L	45 mg/L	89 mg/L
Ramo 16[a]	β-Ketoacyl reductase	3.6 mg/L	—	11.5 mg/L
Ramo 17[a]	NRPS	n. d.	n. d.	5.6 mg/L[d]
Ramo 24[a]	Dehydrogenase	n. d.	n. d.	×<1 mg/L [d]
Ramo 24[b]		n. d.	n. d.	—
Ramo 25[a]	Dehydrogenase	n. d.	n. d.	n. d.
Ramo 25[b]		n. d.	n. d.	—
Ramo 26[a]	Acyl-CoA ligase	4.6 mg/L	10 mg/L	81 mg/L
Ramo 26[b]		45 mg/L	112 mg/L	—
Ramo 27[a]	MbtH-like protein	120 mg/L	288 mg/L	315 mg/L

[a] Expressed in *E. coli* BL21 DE3 cells.
[b] Expressed in *E. coli* BL21 DE3-RP cells.
[c] Not detected.
[d] Enzyme precipitation observed over time.

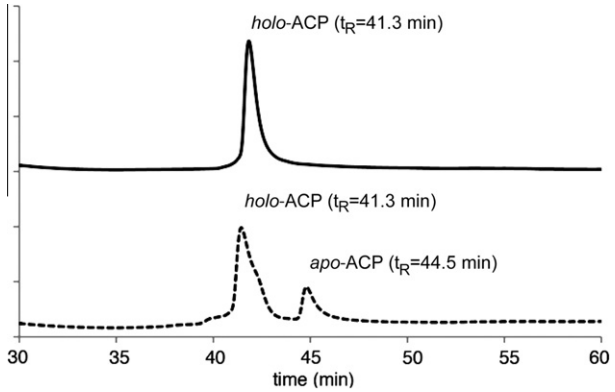

Figure 3. HPLC analysis of Ramo 11 incubated in the absence (dashed line) and presence (solid line) of the phosphopantetheinyl transferase enzyme Sfp, ATP, and Coenzyme A. Peaks corresponding to the retention time of the holo-form (t_R = 41.3) and apo-form (t_R = 44.5 min) were collected and confirmed for composition by MALDI-TOF mass analysis. The Y axis is a stacked overlay of two traces, but represents data in absorbance units, scaled identically for each trace.

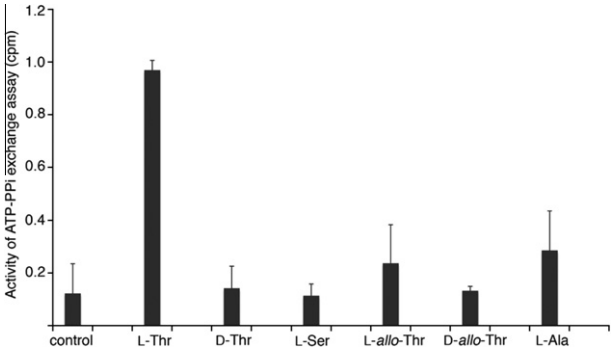

Figure 4. Ramo 17 ATP-PPi exchange assay. Shown are two replicate purifications, each sample assayed in triplicate where the amino acid incubated with the enzyme was compared against a control of no amino acid. Data was normalized to the most active amino acid.

subtilis phosphopantetheinyl transferase Sfp. Sfp has an unusually promiscuous substrate specificity profile, recognizing the conserved fold of ACPs and efficiently transferring phosphopantetheine cofactors to an evolutionarily conserved serine.[30] When treated with Sfp, Ramo 11 was quantitatively converted to the *holo* form as judged by HPLC analysis, MALDI-TOF mass spectrometry, and protein sequencing (Fig. 3). These data confirm the predicted acyl carrying function of Ramo 11 and also indicate that the recombinantly produced protein is correctly folded since it was an efficient substrate for Sfp.

2.4. Confirmation of the activity of the standalone NRPS Ramo 17

Ramo 17, a 95 kDa protein, is an unusual standalone NRPS encoding an external domain of unknown function, an adenylation domain hypothesized to activate L-*allo*-threonine, and a thiolation domain.[14,19,20] To determine if Ramo 17 was folded correctly following expression in the presence of *S. lividans* GroES/GroESL1, two assays were conducted to measure the capacity of Ramo 17 to be phosphopantetheinylated by Sfp, and also for this enzyme to produce aminoacyl adenylates.

Ramo 17 was first incubated with Sfp and BODIPY-CoA, a fluorescently labeled Coenzyme A analog.[31] Like acyl carrier proteins, NRPS thiolation domains contain the phosphopantetheinyl cofactor, which is used for module-to-module transfer of the growing peptides on the NRPS. When analyzed by denaturing polyacrylamide gel electrophoresis and illuminated under fluorescent light, the band corresponding to Ramo 17 exhibited fluorescence, indicative of transfer of the BODIPY fluorophore covalently to the thiolation domain of Ramo 17 (data not shown). These data indicate that the thiolation domain within Ramo 17 was correctly folded and thus could be modified by Sfp.

Second, to determine if the adenylation domain of Ramo 17 was correctly folded and enzymatically active, the specificity of the adenylation domain was probed by ATP–PPi exchange assay using a variety of amino acids as substrates. Ramo 17 is responsible for the addition of the eighth residue in ramoplanin, L-*allo*-threonine. Since there is less available sequence and structural data from Thr-specific adenylation domain pockets, it is difficult determine *a priori* which amino acid, L-*allo*-threonine or L-threonine, is the preferred substrate based on sequence analysis alone.[19,20] We tested Ramo 17 for ATP–PPi exchange as a measure of adenylation activity using a panel of amino acids. The data showed that Ramo 17 preferentially activates L-threonine, and to a lesser extent L-alanine and L-*allo*-threonine (Fig. 4). Intriguingly L-*allo*-threonine appears in the natural product but was utilized by Ramo 17 with approximately 25% of the efficiency of L-threonine. The absence of internal epimerization domains within all four biosynthetic NRPS enzymes and a lack of a stand alone epimerase gene within the remaining genes within the locus suggests that L-threonine incorporation followed by epimerization at the beta carbon is a remote possibility. Instead, a more plausible mechanism by which L-*allo*-threonine is preferentially incorporated might be a result of the availability of the amino acid pool within the *Actinoplanes* host producer. Collectively, these data underscore the importance that co-expression with *S. lividans* GroES/GroEL1 chaperones markedly enhance both the production of soluble Ramo 17 and produce folded protein capable of dual activities as a substrate for phosphopantetheinyl transfer and as an enzyme capable of aminoacylation.

2.5. Confirmation of Ramo 16 as an NADH-dependent reductase

As mentioned previously, Ramo 16 is a putative NADH dependent reductase with homology to the type II fatty acid biosynthesis NADPH-dependent reductase FabG. Successful expression of Ramo 16 with a C-terminal hexahistidine tag was accomplished, however immediate unrecoverable precipitation of Ramo 16 occurred upon affinity purification. A variety of techniques were utilized to overcome this precipitation, however, none successfully stabilized the protein. Due to protein instability caused by adding N- or C-terminal affinity purification hexahistidine sequences to the Ramo 16 sequence, the enzyme was prepared as a full-length native protein sequence by co-expression with GroESL chaperones in autoinduction media. Following purification to near homogeneity, to examine if this enzyme was folded correctly, we monitored Ramo 16 for reductase activity in a continuous spectrophotometric assay in the presence of NADH and a pseudo-substrate acetoacetyl-Coenzyme A, a mimic for the 3-oxoacyl-acyl carrier protein substrate believed to be composed of the *N*-acyl fatty acid and Ramo 11. Ramo 16 catalyzed the formation of 3-hydroxybutyryl Coenzyme A from acetoacetyl-Coenzyme A with the following kinetic parameters for acetoacetyl-Coenzyme A: K_M of 2350 ± 390 μM and a k_{cat} of 15.7 ± 1.2 s^{-1} at a fixed concentration 250 μM NADH (Fig. 5). Although without chaperones, Ramo 16 expressed at 3.6 mg/L, the preparations were of low specific activity. Expression in the presence of chaperones increased the soluble yield to >11 mg/L, but more importantly the specific activity was markedly improved.

The GroES/GroEL chaperonins and their effect on protein folding have been extensively demonstrated, mainly for expression of mammalian enzymes within bacterial heterologous hosts.

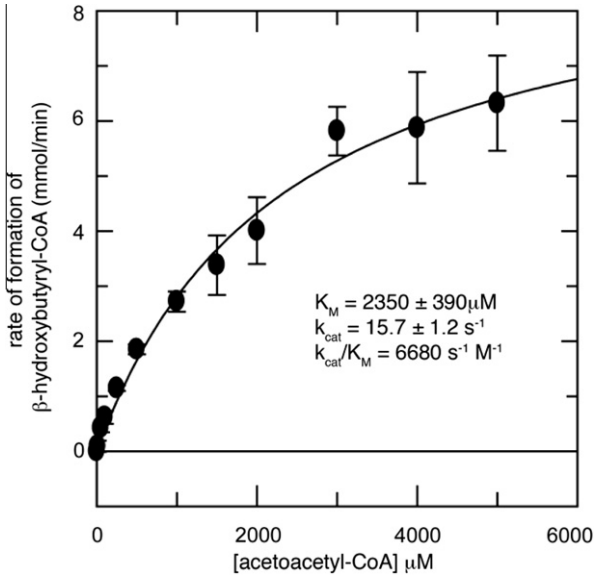

Figure 5. Kinetic profile and kinetic parameters of Ramo 16 (10 μM) with varied acetoacetyl-CoA (0–5 mM) and fixed NADH concentrations (250 μM).

Although it appears that many of these large NRPSs are too large to fit in the predicted cavity of the GroEL barrel, it may be possible to explain this folding assistance by an alternate model.[24,26,32,33] The GroEL barrel may function without GroES, its 10 kDa subunit that forms the cap on the barrel during protein folding. This mechanism is not unprecedented, prior experiments by the laboratory of Chaudhuri have found a protein that requires both GroES and GroEL for proper folding[34,35] and yet is predicted to be too large to be accommodated within the GroEL binding pocket. An alternate mechanism of folding was proposed to explain this anomaly.[35] If the GroEL barrel functions without the GroES cap sealing the cavity, then it is possible that each domain or portion of a domain may assist in its localized folding prior to release.

3. Conclusion

In summary, we have applied chaperone-assisted protein expression to the successful production of ramoplanin biosynthesis-associated proteins and have confirmed function and/or kinetic parameters for a representative set of gene products, confirming biological functions predicted from sequence. This advance now makes possible the detailed mechanistic and structural characterization of enzymes within this antibiotic class, and may be broadly applicable to the production and reconstitution of active enzymes from natural product biosynthetic gene products that have proved refractory by conventional means. Genes from the ramoplanin biosynthetic locus have been historically difficult to produce, and this approach now paves the way for understanding important aspects of its construction, including assembly of the starter unit and other intriguing sequence, structure and functional features of enzymes from this gene cluster in preparation for potential metabolic engineering applications.

4. Experimental

4.1. Materials and general methods

Enzymes required for DNA manipulations were obtained from New England Biolabs. Herculase HotStart was purchased from Stratagene. The ZeroBlunt Cloning kit was purchased from Invitrogen. [^{32}P]-Labeled inorganic pyrophosphate was acquired from NEN. Media, supplements, and antibiotics were purchased from Sigma and Difco. *E. coli* competent cells were obtained from Invitrogen and Stratagene. Expression plasmids (pET30b, pET16b) and cloning plasmids (pLacI) were purchased from Novagen. Centricon concentrators were acquired from Amicon. HALT protease inhibitors were purchased from Pierce. EconoPac DG 10 desalting columns were purchased from Bio-Rad. All other chemicals were reagent grade and purchased from VWR or Sigma–Aldrich. The cosmids containing the ramoplanin biosynthetic cluster (008CK, 008CO) were gifts from Dr. Chris Farnet (Ecopia Biosciences). The plasmid pGroESL was a gift from Prof. George Lorimer (Univ. of Maryland). BODIPY-CoA and the enzyme Sfp were gifts from Prof. Christopher Walsh (Harvard Medical School). FPLC purifications were performed on an AKTA FPLC from GE Healthcare. Cell lysis was performed on an Avestin Emulsiflex C-5 homogenizer. HPLC purifications were performed on an Agilent 1200 HPLC. Centrifugation was performed on a Beckman Coulter Optima LE-80K Ultra centrifuge. Absorbance measurements were obtained on a HP 8453 UV–visible spectrophotometer. Scintillation counting was performed using a Wallac 1209 rack beta counter. MALDI-TOF mass spectrometry analysis was performed on an Applied Biosystems Voyager System 6154 instrument.

4.2. Cloning, Expression, and Purification of Ramo 9, Ramo 11, Ramo 12, Ramo 15, Ramo 17, Ramo 24, Ramo 25, Ramo 26, and Ramo 27 Proteins into *E. coli*

PCR amplification was performed on the cosmid 008CK with the following primers : Ramo9F (5′-ggg aat tcc ata tga gcg ccg cgg gct ccg gtt-3′); Ramo9R (5′-ccc aag ctt gtg gga gtc gag gaa ctc gag gat-3′), Ramo15R (5′-CCC AAG CTT GTC ACG GTC CAG GTC GGC GGC GAT-3′); Ramo15F (5′-GGG AAT TCC ATA TGC AGA AGA TCC CGC TCG TGT-3′); Ramo17F (5′-CAT ACA TAT GCC CAA GTC CCA GCC CGC C-3′); Ramo17R (5′-CAT AAA GCT TGG CCG AGC GCA ACG C-3′); Ramo24F (5′-GGG AAT TCC ATA TGA CCG CCG CGG CGC TCG AGA AGC-3′); Ramo24R (5′-CCC AAG CTT GCC GGG GAG CTG ACG GGC GCT CAG G-3′); Ramo25F (5′-GGG AAT TCC ATA TGA CCG TAC GCC CGC TGG CGC CAC-3′); Ramo25R (5′-CCC AAG CTT CCG GCC GTC CTC CGC CCG GAC GGT G-3′); Ramo26F (5′-ggg aat tcc ata tgg tca tcg acg ccg cca ccc aac-3′); Ramo26R (5′-CCC AAG CTT TCG GCC CGC GCC CGC CTG CAC CGG C-3′); Ramo27F (5′-ggg aat tcc ata tgc cca atc cgt ttg aag atc ccg-3′); Ramo27R (5′-CCC AAG CTT GCT CTG CGG TTG CTT CTG CTT CTC C-3′); Ramo11F (5′-GGG AAT TCA TAT GTC CGA GAC CGA CCT GTC C-3′); Ramo11R (5′-TAT AAA GCT TTT ATC GGT TGA CGC GGT CGG C-3′). The PCR amplification was optimized for each gene. Typical reaction conditions and cycle consisted of 98 °C for 5 min, 98 °C for 45 s, 57 °C for 45 s, 72 °C for 6 min (last three temp cycles repeated 30X), and 72 °C for 10 min. The PCR mixture consisted of Herculase Hot-Start polymerase, supplied buffer, dNTP mix, primers, 9% DMSO, and cosmid DNA. PCR products were gel purified and ligated into the Zero Blunt Cloning vector.

Successful ligations were sequenced and constructs containing the correct gene sequence were excised and ligated into pET30b with *Nde*I and *Hind*III restriction sites. The pET30b constructs containing the gene of interest were transformed into BL21 (DE3) cells at 23 °C. The cultures were induced with 100 μM IPTG when the optical density at 600 nm reached 0.6 and allowed to grow overnight. Cells were pelleted and frozen at −20 °C until needed. The cells were centrifuged (3600*g* for 10 min and resuspended in buffer A (50 mM Tris–HCl, pH 8.0, 300 mM NaCl, 10 mM imidazole). The cells were lysed by multiple passages through the Emulsiflex. The slurry was centrifuged at 125,000*g* for 45 min and loaded onto a pre-equilibrated nickel-chelating column. The column was washed with 250 mL of buffer A and then subjected to a linear gradient to 100% buffer B (50 mM Tris–HCl, pH = 8.0, 300 mM NaCl,

500 mM imidazole). Fractions exhibiting an absorbance at 280 nm were analyzed by SDS–PAGE and fractions containing purified proteins were pooled. The proteins were excised from the acrylamide gel and subjected to trypsin digest and analysis by Q-TOF to confirm identity. Values for the total production of purified proteins were obtained by Bradford analysis against bovine serum albumin standards. Co-transformations involving pGroESL (exhibiting ampicillin resistance) and pLacI-GroESEL (chloramphenicol resistance) were purified similarly with the additional antibiotic present during bacterial growth.

4.3. Cloning of GroESEL1

Genomic DNA from *S. lividans* was prepared as previously described.[36] The PCR mixture and conditions were similar to the previously described reaction. The primers were GroESEL forward 5′-GCA CCC GCG ACG ACG GAT CCA C-3′, GroESEL reverse 5′-TCA GTG GGA GTG GCC TAG GTG GCT GTG-3′. PCR products were ligated into the Zero Blunt Cloning vector and confirmed by DNA sequencing, the insert was excised by digestion with *Eco*RI, then blunted with Klenow fragment (DNA polymerase I). The pLacI vector was digested with *Bsa*AI and dephosphorylated with Antarctic Phosphatase. The vector and insert were ligated and transformed into DH5α cells. Transformants were screened for insert and orientation by restriction digest and confirmed by DNA sequencing.

4.4. Cloning and purification of Ramo 16

The Ramo 16 gene was obtained by PCR amplification from cosmid DNA (OO8CK) from *Actinoplanes* ATCC 33076 using Herculase Hot Start Polymerase with the following primers: the C-terminal his-tag were Ramo16C forward (5′-GGG AAT TCC ATA TGC gct tga ccg gca aga ccC CG-3′), Ramo16C reverse (5′-ccc aag ctt gcg cgt ggt gaa tcc gcc gtc gac-3′), and the N-terminal hexahistidine-tag were Ramo16N forward (5′-TAT ACC ATG GCT CGC TTG ACC GGC AAG AC-3′). and Ramo16N reverse (5′-TAT AGG ATC CTC AGC GCG TGG TGA ATC CG-3′). The amplified gene products were cloned into the Zero Blunt Cloning Vector and sequenced. The Ramo 16 insert was digested out of the vector with either *Nde*I and *Hind*III or *Nco*I and *Bam*HI for the C-terminal and N-terminal hexahistidine-tag constructs, respectively. The inserts were ligated into pET30b expression vector to create pET30b-ramo16C and pET30b-ramo16N. Each plasmid was transformed into BL21 (DE3) for expression. pET30b-ramo16N did not yield any soluble protein. pET30b-ramo16C yielded soluble protein, however, the protein was markedly unstable and inactive. The N-terminal portion of pET30b-ramo16C was digested and ligated into the identically cut C-terminal portion of the pET30b-ramo16N to yield pET30b-ramo16-native. Containing no fusion tag, this native protein, was sequenced and then transformed into BL21 (DE3) cells for expression.

An overnight culture was grown in Luria broth with kanamycin (50 μg/mL), diluted 1:100 into auto-induction media[37] and grown at 23 °C for 48 h. Cells were harvested and suspended in Tris (50 mM, pH 8.0) supplemented with DTT (1 mM) and HALT protease inhibitors. Lysis was performed with three passages through the Emulsiflex and centrifuged (125,000*g* for 45 min). Clarified lysate was applied to a Q sepharose column and eluted with a gradient (300 mL) of 0–350 mM NaCl in the above buffer without protease inhibitors. Fractions containing Ramo 16 were pooled and concentrated and applied to a Superdex S-200 column pre-equilibrated with Tris (50 mM, pH = 8.0), NaCl (100 mM) and DTT (1 mM). Fractions were analyzed by SDS–PAGE and the band corresponding to Ramo16 was excised and the identity of the protein confirmed by Q-TOF. Fractions containing Ramo 16 were pooled, concentrated, flash frozen and stored at −80 °C.

4.5. Assay of Ramo 16 reductase activity

Initial rates of Ramo 16 were determined by monitoring the decrease in absorbance of NADH at 340 nm at 25 °C. The reactions (100 μL) were monitored in half-area clear bottom Corning plates using a 96 well plate SpectraMax Molecular Devices spectrophotometer. The extinction coefficient for NADH at 340 nm for 100 μL reactions was 3296 M^{-1}.[38] Assays were performed in HEPES (50 mM pH 7.6), NaCl (100 mM), and Ramo 16 (10 μM). Initial rates were measured over the first 300 s. Rates were determined by varying acetoacetyl-CoA (0–5 mM) while NADH was held constant (250 μM).

4.6. Phosphopantetheinylation of Ramo 11 by Sfp

Purified Ramo 11 (40 μM) was incubated for 1 h with purified Sfp (5 μM) in HEPES buffer (50 mM, pH 7.0) with $MgCl_2$ (2 mM) and Coenzyme A (100 μM). The reaction and a control without Sfp were subjected to HPLC analysis on a linear gradient of H_2O (containing 0.1% TFA) to MeOH (containing 0.1% TFA) on octadecyl silica column (Vydac C_{18} 4.6 × 250 mm). Apo-ACP possessed identical properties as commercial standards and successfully converted to the holo-ACP upon experimental incubation. Samples collected at the expected retention time (holo-ACP t_R = 41.3 min) were subjected to MALDI-TOF MS analysis and showed masses consistent with holo-ACP (theoretical (m/z) = 13,014 Da; experimental holo-ACP (m/z) = 13,010 Da).

4.7. Purification of Ramo 17 and assay of ATP-PPi exchange activity

Ramo 17 containing a C-terminal hexahistidine affinity tag was concentrated with a 30 kDa molecular weight cutoff Centricon concentrator, loaded onto a desalting column for imidazole removal and eluted with 50 mM Tris, pH 8.0 (4 mL), 50 mM NaCl. A modification of the method of Du et al. was used for analysis of PPi exchange.[30,39,40] The protein was incubated for 30 min in 50 mM sodium phosphate, pH 7.8, 1 mM ATP, 0.2 μCi/1 mM [^{32}P]-PPi, 1 mM $MgCl_2$, 0.2 mM EDTA, and 1 mM amino acid (L-threonine, D-threonine, D-*allo*-threonine, L-*allo*-threonine, L-alanine, L-serine, or a control with ddH_20) at 25 °C. The reaction was quenched in 1% activated charcoal and 3% perchloric acid and bound to a glass fiber filter. The filter was sequentially washed with sodium phosphate, (0.2 M, pH 8.0), H_2O, and finally ethanol. The dried filter was analyzed by scintillation counting. All experiments were performed in triplicate.

4.8. Assay for covalent labeling of Ramo 17 by BODIPY-CoA

Purified Ramo 17 (40 μM) was incubated for 1 h with purified Sfp (5 μM) in HEPES buffer (50 mM, pH = 7.0) with $MgCl_2$ (2 mM), Coenzyme A (100 μM), and BODIPY-CoA (40 μM).[31] The reaction and a control without Sfp were analyzed by denaturing 10% gel SDS–PAGE then imaged with fluorescence detection or by direct Coomassie staining.

Acknowledgments

This work was supported by National Institutes of Health research grant AI46611 (to D.G.M.). Amanda Hoertz is the recipient of a Zeilik Fellowship. Dr. James B. Hamburger is a Crohns and Colitis Foundation Postdoctoral Fellow

Supplementary data

Supplementary data (SDS–PAGE images of purified proteins) associated with this article can be found, in the online version, at doi:10.1016/j.bmc.2011.11.062.

References and notes

1. Neu, H. C.; Neu, N. M. *Chemotherapy* **1986**, *32*, 453.
2. Cavalleri, B.; Pagani, H.; Volpe, G.; Selva, E.; Parenti, F. *J. Antibiot. (Tokyo)* **1984**, *37*, 309.
3. Pallanza, R.; Berti, M.; Scotti, R.; Randisi, E.; Arioli, V. *J. Antibiot. (Tokyo)* **1984**, *37*, 318.
4. Pallanza, R.; Scotti, R.; Beretta, G.; Cavalleri, B.; Arioli, V. *Antimicrob. Agents Chemother.* **1984**, *26*, 462.
5. Biavasco, F.; Manso, E.; Varaldo, P. E. *Antimicrob. Agents Chemother.* **1991**, *35*, 195.
6. Finegold, S. M.; John, S. S.; Vu, A. W.; Li, C. M.; Molitoris, D.; Song, Y.; Liu, C.; Wexler, H. M. *Anaerobe* **2004**, *10*, 205.
7. Johnson, C. C.; Taylor, S.; Pitsakis, P.; May, P.; Levison, M. E. *Antimicrob. Agents Chemother.* **1992**, *36*, 2342.
8. Jones, R. N.; Barry, A. L. *Diagn. Microbiol. Infect. Dis.* **1989**, *12*, 279.
9. Mobarakai, N.; Quale, J. M.; Landman, D. *Antimicrob. Agents Chemother.* **1994**, *38*, 385.
10. Pelaez, T.; Alcala, L.; Alonso, R.; Martin-Lopez, A.; Garcia-Arias, V.; Marin, M.; Bouza, E. *Antimicrob. Agents Chemother.* **2005**, *49*, 1157.
11. Ristow, T. A.; Noskin, G. A.; Warren, J. R.; Peterson, L. R. *Microb. Drug Resist.* **1995**, *1*, 335.
12. Rolston, K. V.; Dholakia, N.; Ho, D. H.; LeBlanc, B.; Dvorak, T.; Streeter, H. J. *Antimicrob. Chemother.* **1996**, *38*, 265.
13. Fang, X.; Tiyanont, K.; Zhang, Y.; Wanner, J.; Boger, D.; Walker, S. *Mol. Biosyst.* **2006**, *2*, 69.
14. Fang, X.; Nam, J.; Shin, D.; Rew, Y.; Boger, D. L.; Walker, S. *Bioorg. Med. Chem. Lett.* **2009**, *19*, 6189.
15. Farnet, C. M.; Zazopoulos, E.; Staffa, A., US Patent Number 0164747, **2002**.
16. Marahiel, M. A.; Stachelhaus, T.; Mootz, H. D. *Chem. Rev.* **1997**, *97*, 2651.
17. Cane, D. E.; Walsh, C. T. *Chem. Biol.* **1999**, *6*, R319.
18. von Dohren, H.; Keller, U.; Vater, J.; Zocher, R. *Chem. Rev.* **1997**, *97*, 2675.
19. Challis, G. L.; Ravel, J.; Townsend, C. A. *Chem. Biol.* **2000**, *7*, 211.
20. Stachelhaus, T.; Mootz, H. D.; Marahiel, M. A. *Chem. Biol.* **1999**, *6*, 493.
21. McCafferty, D. G.; Cudic, P.; Frankel, B. A.; Barkallah, S.; Kruger, R. G.; Li, W. *Biopolymers* **2002**, *66*, 261.
22. Mootz, H. D.; Schwarzer, D.; Marahiel, M. A. *ChemBioChem* **2002**, *3*, 490.
23. Yin, X.; Zabriskie, T. M. *Microbiology* **2006**, *152*, 2969.
24. Betancor, L.; Fernandez, M. J.; Weissman, K. J.; Leadlay, P. F. *ChemBioChem* **2008**, *9*, 2962.
25. Cole, P. A. *Structure* **1996**, *4*, 239.
26. Walter, S.; Buchner, J. *Angew. Chem., Int. Ed.* **2002**, *41*, 1098.
27. Horwich, A. L.; Farr, G. W.; Fenton, W. A. *Chem. Rev.* **2006**, *106*, 1917.
28. Thirumalai, D.; Lorimer, G. H. *Annu. Rev. Biophys. Biomol. Struct.* **2001**, *30*, 245.
29. Martin, J. *Biochemistry (Mosc)* **1998**, *63*, 374.
30. Ku, J.; Mirmira, R. G.; Liu, L.; Santi, D. V. *Chem. Biol.* **1997**, *4*, 203.
31. La Clair, J. J.; Foley, T. L.; Schegg, T. R.; Regan, C. M.; Burkart, M. D. *Chem. Biol.* **2004**, *11*, 195.
32. Paul, S.; Singh, C.; Mishra, S.; Chaudhuri, T. K. *FASEB J.* **2007**, *21*, 2874.
33. Gupta, P.; Aggarwal, N.; Batra, P.; Mishra, S.; Chaudhuri, T. K. *Int. J. Biochem. Cell. Biol.* **2006**, *38*, 1975.
34. Dubaquie, Y.; Looser, R.; Funfschilling, U.; Jeno, P.; Rospert, S. *EMBO J.* **1998**, *17*, 5868.
35. Chaudhuri, T. K.; Farr, G. W.; Fenton, W. A.; Rospert, S.; Horwich, A. L. *Cell* **2001**, *107*, 235.
36. Hopwood, D. A.; Bibb, M. J.; Chater, K. F.; Kieser, T.; Bruton, C. J.; Kieser, H.; Lydiate, D. J.; Smith, C. P.; Ward, J. M.; Schrempf, H. *Genetic Manipulation of Streptomyces: a Laboratory Manual*; John Innes Foundation: Normiwch, 1985.
37. Studier, F. W. *Protein Expr. Purif.* **2005**, *41*, 207.
38. Percival, M. D. *Anal. Biochem.* **2003**, *313*, 307.
39. Lee, S. G.; Lipmann, F. *Methods Enzymol.* **1975**, *43*, 585.
40. Du, L.; Shen, B. *Chem. Biol.* **1999**, *6*, 507.